HHS Public Access

Author manuscript

Chem Res Toxicol. Author manuscript; available in PMC 2020 April 15.

Published in final edited form as:

Chem Res Toxicol. 2019 April 15; 32(4): 727–736. doi:10.1021/acs.chemrestox.8b00389.

Toxicokinetics of Chiral PCB 136 and its Hydroxylated Metabolites in Mice with a Liver-Specific Deletion of Cytochrome P450 Reductase

Xueshu Li[†], **Xianai Wu**[†], **Kevin M. Kelly**[†], **Peter Veng-Pedersen**[‡], and **Hans-Joachim Lehmler**[†,*]

[†]Department of Occupational and Environmental Health, College of Public Health, University of Iowa, Iowa City, IA 52242

[‡]College of Pharmacy, University of Iowa, Iowa City, IA 52242

Abstract

Exposure to polychlorinated biphenyls (PCBs) has been implicated in adverse human health effects, including developmental neurotoxicity. Several neurotoxic PCBs are chiral and undergo atropisomeric enrichment *in vivo* due to atropselective metabolism by cytochrome P450 enzymes. Here we study how the liver-specific deletion of the cytochrome P450 reductase (*cpr*) gene alters the toxicokinetics of 2,2',3,3',6,6'-hexachlorobiphenyl (PCB 136) in mice. Male and female mice with a liver-specific deletion of *cpr* (KO) and congenic wild-type (WT) mice were exposed to a single oral dose of racemic PCB 136 (6.63 mg/kg). Levels and chiral signatures of PCB 136 and its hydroxylated metabolites were determined 1 to 48 h after PCB exposure in whole blood. Blood levels of PCB 136 were typically higher in M-WT compared to F-WT mice. At the later time points, F-KO mice had significantly higher PCB 136 levels than F-WT mice. 2,2′,3′,4,6,6′-Hexachlorobiphenyl-3-ol (3–150), 2,2′,3,3′,6,6′-hexachlorobiphenyl-4-ol (4–136), 2,2′,3,3′,6,6′-hexachlorobiphenyl-5-ol (5–136) and 4,5-dihydroxy-2,2′,3,3′,6,6′-hexachlorobiphenyl (4,5–136) were detected in blood, with 5–136 and 4–136 being major metabolites. At later time points, the sum of HO-PCB (ΣHO-PCB) levels exceeded PCB 136 levels in the blood; however, higher ΣHO-PCB than PCB 136 levels were observed later in KO than WT mice. PCB 136 and its major metabolites displayed atropisomeric enrichment in a manner that depended on the time point, sex and genotype. Toxicokinetic analysis revealed sex and genotype-dependent differences in toxicokinetic parameters for PCB 136 atropisomers and its metabolites. The results suggest that mice with a liver-specific deletion of the *cpr* gene can potentially be used to assess how an altered metabolism of neurotoxic PCB congeners affects neurotoxic outcomes following exposure of the offspring to PCBs via the maternal diet.

[*]**Corresponding Author** hans-joachim-lehmler@uiowa.edu. Phone: +1-319-335-4981.

ASSOCIATED CONTENT

Supporting Information

The supporting information includes tables with wet tissue weight and body weight; method detection limits, limits of detection and limits of quantification; toxicokinetic parameters; EF values of PCB 136 and hydroxylated metabolites in whole blood; and a comparison of selected toxicokinetic parameters of PCB 136 and its metabolites in KO and. WT mice exposed orally to racemic PCB 136. This material is available free of charge via the Internet at http://pubs.acs.org

Notes

The authors declare no competing financial interest.

Graphical Abstract

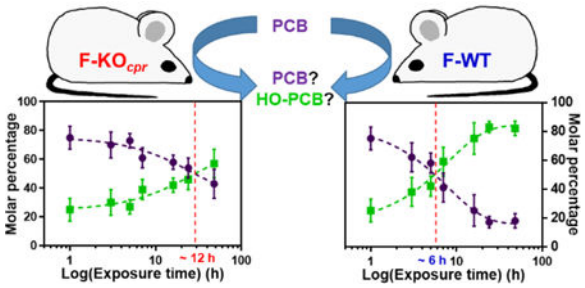

INTRODUCTION

PCBs are persistent organic pollutants listed on the Substance Priority List of the United States Agency for Toxic Substances and Disease Registry.[1] Chemicals on this list represent a significant human health concern and are commonly found at Superfund hazardous waste sites. The production of PCBs is banned globally under the Stockholm Convention; however, PCBs can be used until 2025 in enclosed applications, but need to be eliminated by 2028.[2] Besides, PCBs are formed as industrial byproducts and, as a consequence, are present in consumer products, including paints and polymer resins.[3–5] The production and widespread use of PCBs has resulted in ubiquitous global contamination of water, soil, plants, wildlife and humans.[6,7] PCBs are not only present in the diet,[8–10] but also in outdoor air and indoor air of schools,[11–16] thus raising concerns about both dietary and inhalation exposures to these compounds.[16–18]

Epidemiological findings consistently demonstrate an association between developmental exposure to environmental PCBs and deficits in measures of neurophysiological function in infancy and childhood.[19–21] In animal studies, both technical PCB mixtures and individual PCB congeners cause adverse neurotoxic outcomes following developmental PCB exposure of the offspring via the diet of the dam.[22–24] It is noteworthy that PCB congeners with multiple *ortho* chlorine substituents recapitulate the developmental neurotoxicity of technical PCB mixtures, such as Aroclor 1254,[22,23] an observation that implicates these congeners in PCBs' developmental neurotoxicity. Several mechanisms are proposed to mediate PCB developmental neurotoxicity, including altered calcium homeostasis in the developing brain.[25] Ryanodine receptor (RyR)-dependent modulation of calcium signaling pathways has emerged as a key mechanism by which PCB congeners with multiple *ortho* substituents affect neural connectivity in rodent models.[22,26]

PCB 136 is an environmentally relevant PCB congener that displays axial chirality due to the hindered rotation around the phenyl-phenyl bond.[27] Like structurally related PCB congeners, PCB 136 is readily absorbed by passive diffusion from the gastrointestinal tract[27] and metabolized by cytochrome P450 enzymes in the liver and, possibly, other organs to hydroxylated metabolites (OH-PCBs; Figure 1).[13,27] Animal studies suggest that both mono- and dihydroxylated metabolites of PCB 136 are present in the postnatal mouse brain following developmental exposure via the maternal diet.[28] Importantly, levels of OH-PCB 136 metabolites in the postnatal brain are comparable to the levels of the parent compound.

Analogous to the parent PCBs, OH-PCB metabolites, including metabolites of PCB 136, also alter cellular calcium signaling by activating RyRs.[29,30] Exposure of postnatal mice to PCB 136 via the maternal diet changes the expression of neural plasticity and thyroid hormone-responsive genes *in vivo*. Taken together, these observations raise the question if the atropselective oxidation of PCB136 and structurally related PCB congeners plays a role in their developmental neurotoxicity;[28] however, studies linking the metabolic activation of PCBs to neurotoxic outcomes have not been reported in the literature to-date.

Transgenic animal models with altered metabolism of neurotoxic PCBs congeners can potentially be used to study the role of hepatic metabolism in PCB developmental neurotoxicity. KO mice with a liver-specific deletion of the cytochrome P450 oxidoreductase (*cpr*) gene are one mouse model that is of particular interest in this context. KO mice have an impaired hepatic metabolism because CPR, the required electron donor for microsomal cytochrome P450 enzymes, is not expressed in the liver.[31,32] A preliminary study demonstrated that the disposition of PCB 136 and its metabolites is significantly altered in female KO (F-KO) compared to congenic female wild-type mice (F-WT).[33] The present study provides an in-depth investigation of the toxicokinetics of PCB 136 and its major hydroxylated metabolites (OH-PCBs) in male and female KO vs. WT mice to explore if CPR-null mice can be used for studies linking PCB metabolism to neurotoxic outcomes following developmental exposure via the dam.

EXPERIMENTAL PROCEDURES

Chemicals.

2,3,4’,5,6-Pentachlorobiphenyl (PCB 117, recovery standard), 2,2’,3,4,4’,5,6,6’-octachlorobiphenyl (PCB 204, internal standard) and 2,3,3’,4,5,5’-hexachlorobiphenyl-4’-ol (4’−159, internal standard) were purchased from Accustandard (New Haven, CT, USA). 2,2’,3,3’,6,6’-Hexachlorobiphenyl (PCB 136) and analytical standards of the corresponding hydroxylated PCB metabolites, 2,2’,3’,4,6,6’-hexachlorobiphenyl-3-ol (3–150), 2,2’,3,3’,6,6’-hexachloro-biphenyl-4-ol (4–136), 2,2’,3,3’,6,6’-hexachlorobiphenyl-5-ol (5–136), and 4,5-dimethoxy-2,2’,3,3’,6,6’-hexachlorobiphenyl (4,5–136) were prepared as described elsewhere.[34,35] The chemical structure and corresponding abbreviations are shown in Figure 1. Diazomethane for the derivatization of hydroxylated PCBs to methoxylated PCBs was synthesized from *N*-methyl-*N*-nitroso-*p*-tolulenesulfonamide (Diazald) using an Aldrich mini Diazald apparatus (Milwaukee, WI, USA).[36]

Mouse model maintenance and characterization.

Alb-Cre$^{+/-}$/Cpr$^{lox+/+}$ mice with a liver-specific deletion of the cytochrome P450 oxidoreductase (EC 1.6.2.4) gene (knockout, KO) and congenic Alb-Cre$^{-/-}$/Cpr$^{lox+/+}$ mice (wildtype, WT) were obtained from Dr. Xinxin Ding (University of Arizona, AZ, USA) to establish a breeding colony at the University of Iowa.[31,32] The animal colony was maintained as described.[33] As reported previously, KO mice do not display any CPR activity in the liver, as shown previously in animals from the same colony, and have a fatty liver compared to WT mice.[33] For this study, animals were housed in standard plastic cages in a

temperature controlled room (22 ± 2 °C) with a 12 h light-dark cycle. Basal diet (Harlan 7913 with 18% protein, 6% fat, and 5% fiber) and water were provided *ad libitum.*[33]

Animal exposure.

The Institutional Animal Care and Use Committee of the University of Iowa approved all animal procedures (protocol #: 1206120). Daily animal welfare-assessments were performed by laboratory personnel, and no adverse outcomes were observed throughout the study. The eight-week (8 weeks ± 2 days) old animals were randomly divided into exposure and control group, the exposure group mice were dosed with PCB 136 (6.63 mg/kg body weight; 18.4 μmol/kg body weight) in corn oil (10 mL corn oil/kg body weight) by oral gavage. This dose was selected based on several studies of PCB developmental neurotoxicity that used an equimolar dose of PCB 95 (18.4 μmol/kg body weight),[22,37] a PCB congener that, based on its binding to RyR1,[38] has a similar relative neurotoxic potency as PCB 136.[39] A control group of age-matched mice was dosed with corn oil alone (10 mL corn oil/kg body weight). The animals were euthanized 1, 3, 5, 7, 16, 24 and 48 hours after PCB exposure by asphyxiation with carbon dioxide. Blood was collected by cardiac puncture and stored at glass tubes with 80 μL of ethylenediaminetetraacetic acid solution (EDTA, 7.5% w/w) at −20 °C. Differences in the liver and other tissues weights of wildtype *vs.* knockout mice are consistent with previous reports (Tables S1 and S2).[33]

Extraction of PCB 136 and its metabolites from whole blood.

PCB 136 and its hydroxylated metabolites were extracted with a liquid-liquid extraction method.[40,41] Briefly, surrogate recovery standards (100 ng of PCB 117, and 68.5 ng of 4'-OH PCB 159) were added to each sample, followed by hydrochloric acid (6 M, 1 mL) and 5 mL of 2-propanol. After vortexing for 1 min, the samples were extracted with 5 mL of hexane-methyl *t*-butyl ether (1:1, v/v) and 3 mL of hexane. The combined organic extracts were washed with an aqueous potassium chloride solution (1%, 3 mL). The organic phase was transferred to a new vial, and the aqueous phase was reextracted with 3 mL of hexane. The solvent was evaporated to almost dryness under a gentle stream of nitrogen. The residue was re-dissolved in 2 mL of hexane, and the hydroxylated PCB metabolites were derivatized with 0.5 mL of diazomethane for 16 hours as described previously.[33,35] After derivatization, extracts were subjected to tetrabutylammonium hydrogen sulfate/sodium sulfite and concentrated sulfuric acid clean-up steps before analysis.[33,42]

Gas chromatographic determinations.

Levels of PCB 136 and its hydroxylated metabolites (as methylated derivatives) were determined using an Agilent 6890N gas chromatograph with a ^{63}Ni-μECD detector and a SPB-1 capillary column (60 m length, 250 μm inner diameter, 0.25 μm film thickness, Supelco, St Louis, MO, USA). The following temperature program was used: Hold at 100 °C for 1 min, 5 °C /min to 250 °C and hold at 250 °C for 20 min, 5 °C /min to 280 °C and hold at 280 °C for 3 min. The injector and detector temperatures were 280 °C and 300 °C separately, and the helium flow rate was 1.0 mL/min.[43] Levels of PCB 136 and its metabolites were determined using PCB 204 as internal standard (volume corrector) as described.[33] Raw data for individual animals, average PCB and PCB metabolite levels, and PCBs and OH-PCB levels expressed as mol percent are presented in Datasheets D1-D6.

All enantioselective analyses were performed by headspace solid-phase microextraction (SPME) with a 100 μm polydimethylsiloxane (PDMS) on fused silica fiber (Supelco, Bellefonte, PA, USA) as reported previously.[44] In brief, samples were placed in a glass vial, the solvent was evaporated under a gentle stream of nitrogen, and the head-space was sampled with a 100 μm PDMS fiber (Supelco, Bellefonte, PA, USA) for 60 min at 60 °C, followed by desorption in the injector for 5 min. Atropisomeric analyses of PCB 136 were performed with all samples using an Agilent 7890A gas chromatograph with a ^{63}Ni-μECD detector and a Chiralsil-Dex (CD column, 25 m length, 250 μm inner diameter, 0.25 μm film thickness; Varian, Palo Alto, CA, USA) following a published method with minor modifications.[33,41] The temperature program for atropselective analyses of PCB 136 was: 50 °C, hold at 50 °C for 5 min, 30 °C/min to 90 °C, 30 °C/min to 155 °C and hold for 79 min, 50 °C/min to 225 °C and hold for 15 min.

Enantiomeric fractions of 5–136 and 4–136 were only determined for the 5 h time point because levels of both metabolites were sufficiently high for the atropselective analysis. Atropisomers of 5–136 were separated using a CD column with the following temperature program: 50 °C, hold at 50 °C for 5 min, 15 °C/min to 140 °C and hold for 820 min, 15 °C/min to 225 °C and hold for 10 min. The atropisomers of 4–136 were separated on a CycloSil-B column (CB column, 30 m × 250 μm ID × 0.25 μm film; Agilent, Santa Clara, CA, USA) with the following temperature program: 50 °C, hold at 50 °C for 5 min, 15 °C/min to 160 °C and hold for 340 min, 15 °C/min to 200 °C and hold for 10 min. The injector and detector temperatures were 250 °C for all enantioselective analyses, with a constant helium flow rate of 3.0 mL/min.

Consistent with our earlier studies, the atropisomers of the dihydroxylated metabolite, 4,5–136, did not resolve on either atropselective column.[33,35] To allow a comparison with earlier studies,[35,40,41,43] enantiomeric fractions (EFs) were determined as EF = Area E_2/(Area E_1+Area E_2), where Area E_1 and Area E_2 are the peak areas of the first and second eluting atropisomers, respectively. On both the CD and CB column, the E_1-and E_2-atropisomers of PCB 136 correspond to (−)- and (+)-PCB 136, respectively.[33,45,46] The E_1- and E_2-atropisomers of 5–136 and 4–136 are formed from (−)- and (+)-PCB 136, respectively.[33,41]

Quality Assurance/Quality Control.—The ^{63}Ni-μECDs used for the PCB and HO-PCB analysis were linear up to a concentration of 1000 ng/mL for all analytes investigated (R^2 > 0.999). The detailed summary of the limits of detection, limits of quantification, and background levels of PCB 136 and its metabolites is presented in the supporting material (Table S3). The recoveries of PCB 117 and 4'−159 were 97 ± 9% (range: 78 – 115) and 87 ± 9% (range: 70 – 118) respectively. The resolution of PCB 136, 5–136 and 4–136 were 0.95 ± 0.05 (CD column), 0.85 ± 0.10 (CD column) and 0.88 ± 0.11 (CB column), respectively. EF values for the racemic standards of PCB 136 on CD column, 5–136 on CD column, and 4–136 on CB column were 0.501 ± 0.003 (n = 11), 0.500 ± 0.003 (n = 3), 0.500 ± 0.003 (n = 3), respectively.

Estimation of toxicokinetic parameters.

All toxicokinetic parameters and their variability were determined by Monte Carlo (MC) simulations and are summarized in Table S4. Briefly, MC bootstrap data sampling was done for each of the 24 exposure groups (i.e., six timepoints × wildtype and knockout mice × male and female mice), except for male and female KO mice for which the majority of the 4–136 data were below or near the limit of detection. A total of 100,000 simulations were done for each such group to estimate the expected population toxicokinetic parameter values and their variability (SD) for the group. Although it may be tempting to judge possible differences in parameter values between groups based on means and SDs, this is not a reliable method, especially when dealing with asymmetrical parameter distributions, which is commonly encountered in toxicokinetic studies. The preferred method is the use of quantile intervals in the MC simulations as done in the significance testing in this study.

The following toxicokinetic parameters were determined and are summarized in Table S4: C_{max}, the maximum concentration determined from a single administration, T_{max}, the time when C_{max} is reached; $t_{1/2,}$ the terminal half-life; Cl/F, bioavailability normalized clearance; this parameter can only be determined for the parent compound and depends both on the elimination of the compound, *i.e.*, the clearance (Cl), and the bioavailability (F) resulting from the given route of administration; AUC24, a measure of a single exposure to the compound over a 24 hour period, was determined as the area under the concentration *vs.* time curve in the interval from zero to 24 hours resulting from a single dose given at time zero; AUC24ss, a measure of the exposure to the compound over a 24 hour period at steady state, was determined as the area under the concentration *vs.* time curve at steady state in the interval from zero to 24 hours resulting from a single dose given repeatedly every 24 hours; SSa [SSa = (AUC24ss – AUC24)/AUC24] is the “steady state degree of accumulation” (i.e., the extent of accumulation of the compound in a given tissue) determined from the estimated expectation of individual simulation outcomes. SSa is not calculated from the summary parameter given for AUC24ss and AUC24 because such calculation tends to produce a biased value for SSa. Multiplying SSa by 100, as reported in Table S4, is the expected percent increase in AUC24 in going from single dosing and reaching a steady state when dosing is done repeatedly at 24 h intervals.

Statistical Analyses.—If not stated otherwise, PCB 136 and metabolites data are reported as mean ± standard deviation. Differences in body weights, tissue weights, and EF values were tested with the SAS GLM procedure. These statistical analyses were performed using SAS software.[47] Differences between exposure groups were considered statistically different at $p < 0.05$.

Possible significant difference in toxicokinetic parameters between groups were investigated for the following four pairs: male WT (M-WT) *vs.* F-WT, male KO (M-KO) *vs.* F-KO, M-KO *vs.* M-WT, and F-KO *vs.* F-WT (Table S4) and was done by bootstrap MC sampling the difference in each toxicokinetic parameter between the groups. Significance was determined by comparing the value of the estimated population difference to the $(\alpha/2)100\%$ to $(1-\alpha/2)100\%$ quantile interval determined by the MC simulation with a significance level α of 0.05.

RESULTS AND DISCUSSION

Comparison of PCB 136 levels in whole blood.

PCB 136 was detected in whole blood collected at all time points investigated. No significant differences in PCB 136 levels by genotype or sex were observed 5 h after oral exposure to racemic PCB 136 (Figure 2). However, blood levels of PCB 136 were typically higher in M-WT compared to F-WT mice, a difference that was statistically significant at the 1, 7, 16 and 48 h time points (Datasheet D5). At the later time points, F-KO mice had significantly higher PCB 136 levels than F-WT mice. In an earlier disposition study in the same mouse models, PCB 136 levels in whole blood, as well as adipose tissue, brain liver and feces, were also significantly higher in F-KO compared to F-WT mice, despite the different sampling time point (3 days following exposure) and the higher dose of PCB 136 (30 mg/kg body weight).[33] No significant differences were observed between M-KO and F-KO mice and, with exception of the 1 h time point, M-WT and M-KO mice.

Comparison of OH-PCB levels in whole blood.

Because PCB 136 is oxidized by hepatic and extrahepatic mammalian cytochrome P450 enzymes to potentially toxic mono and dihydroxylated metabolites (reviewed in[48,49]; see Figure 1 for a simplified metabolism scheme), we also measured levels of OH-PCB metabolites. As we suggested previously, extrahepatic metabolism is the likely explanation for the formation of OH-PCB metabolites in KO mice.[33] In earlier disposition studies of PCB 136, both following acute and subchronic oral exposure to PCB 136, OH-PCB levels are frequently lower or at least comparable to PCB 136 levels at the time points and PCB 136 doses investigated.[28,33] In the present study, PCB 136 levels, expressed as the molar percentage, were initially higher compared to the sum of (di)OH-PCB metabolites (ΣOH-PCBs) in all exposure groups (Figure 3). At the later time points, the ΣHO-PCBs exceeded the amount of PCB 136 present in the blood. This change in ΣHO-PCB *vs.* PCB 136 levels occurred much later in the M-KO and F-KO mice compared to the congenic WT mice. The observation that the PCB to PCB metabolite ratios in blood differ between KO and WT mice is caused by several factors, including an impaired hepatic oxidation of PCB 136 to OH-PCBs;[33] compensatory changes in the expression of drug metabolizing organs in the liver and other tissues;[50] and a sequestration of the parent PCB in the fatty liver in KO mice[33] due to the liver-specific deletion of the *cpr* gene. As a consequence, the profile of PCB 136 *vs.* OH-PCBs is expected to differ over time not only in blood but also other target organs depending on the genotype, which in turn may affect toxic outcomes.

In all four exposure groups, 3–150, 5–136, 4–136 and 4,5–136 were detected in whole blood collected at the 5 h time point (Figure 2), whereas several metabolites, in particular, 3–150 in KO mice, were below the detection limit at earlier and/or later time point (for details, see the supporting information). The same four metabolites have been detected in earlier *in vitro* studies using mouse liver microsomes or precision-cut liver tissue slices.[28,33,40] The 1,2-shift product, 3–150, was a minor metabolite detected in whole blood. This metabolite was also detected in earlier studies in the liver, but not blood of WT and KO mice exposed orally to PCB 136.[28,33] Liver microsomes obtained from male C57BL/6 mice formed PCB 136 metabolites in a rank order of 5–136 > 4–136 > 4,5–136. The 1,2-shift product was not

detected in this *in vitro* study.[40] 5–136, 4–136 and 4,5–136 were also detected in whole blood from F-WT and F-KO mice collected 3 days following oral exposure to racemic PCB 136 (30 mg/kg body weight).[33] In a different study, all four PCB 136 metabolites were present in whole blood and tissues, including the brain, from mice exposed throughout gestation and lactation to PCB 136 via the maternal diet.[28] It is important to note that 5–136 is the major metabolite of PCB 136 formed in mice; however, this metabolite is efficiently excreted with the feces.[33]

OH-PCB levels were typically higher in WT compared to KO mice, both for male and female mice (Figures 2, Datasheet D5). For example, these differences between WT and KO mice were statistically significant for 3–150 and 4,5–136 in male mice and 3–150, 5–136, 4–136 and 4,5–136 in female mice at the 5 h time point. Levels of 4,5–136, a potentially redox-active metabolite,[51,52] were significantly higher in M-WT compare to M-KO mice at all time points, with the 24 h time point being the only exception (Datasheet D5). Differences in the levels of 4,5–136 in F-WT compared to F-KO mice were less pronounced and reached statistical significance only at earlier time points. In contrast to male mice, levels of 4,5–136 were not significantly different in F-WT *vs.* F-KO mice at the 48 h time point. Similarly, no significant differences in blood levels of these OH-PCBs were observed between WT and KO mice in our prior study.[33] This observation is not surprising because, as shown in Figure 3, the molar ratios of ∑OH-PCBs to PCB 136 change over time following an acute oral administration of PCB 136 and depend on the genotype and sex.

Atropisomeric enrichment of PCB 136 in whole blood.

The direction and extent of the atropisomeric enrichment of PCB 136 were determined using enantioselective gas chromatography (Figures 4 to 6). E_2-(+)-PCB 136 was enriched in all samples (Figure 4A). EF values were significantly different from the racemic standard at all time points (t-test, $p < 0.05$). The observation that E_2-(+)-PCB 136 is enriched in mice is consistent with other disposition studies reporting the atropisomeric enrichment of PCB 136 in blood samples from mice exposed to racemic PCB 136 alone[28,53,54] or a PCB mixture containing racemic PCB 136.[55,56] The enrichment of E_2-(+)-PCB 136 in this and earlier studies is consistent with a preferential metabolism of E_1-(−)-PCB 136 by hepatic cytochrome P450 enzymes, as observed in *in vitro* metabolism studies.[57] It is important to note that the direction of the atropisomeric enrichment of PCB 136 in mice is significantly different from the enrichment observed in other species, including rats[40,41] and humans.[40] For example, E_1-5–136 and E_1-4–136 were enriched in incubations with mouse liver microsomes, whereas E_2-5–136 and E_2-4–136 were enriched in other species.[40,41]

EF values increased in the 48 hours following exposure to racemic PCB 136, irrespective of sex and genotype (Figure 5; Table S6). The extent of the atropisomeric enrichment of (+)-PCB 136 was more pronounced in WT compared to KO mice for both male and female mice, and EF values were typically significantly higher in WT compared to KO mice for the 3 h to 24 h time points. EF values at the 48 h time point ranged from 0.75 ± 0.02 (M-WT) to 0.78 ± 0.01 (F-WT), and no significant differences between exposure groups were observed at the 48 h time point. For comparison, EF values of PCB 136 were 0.63 ± 0.06 in F-WT mice and 0.66 ± 0.03 in M-WT mice in our prior study with the same mouse model.[33]

Because the extent of the atropisomeric enrichment decreases with increasing dose,[54] the modest differences in the EF values between this and our earlier study are likely due to the higher dose in the earlier study (i.e., 6.63 mg/kg body weight *vs.* 30 mg/kg body weight).

The metabolism of both PCB 136 atropisomers occurs at a lower rate in KO mice due to the impaired hepatic metabolism, thus contributing to the less pronounced atropisomeric enrichment of PCB 136 at the 3 h to 24 h time points (Figure 5). Also, KO animals have a fatty liver due to the deletion of the CPR.[33] As suggested by earlier animal studies, [33,58–60] fatty liver results in a distribution of parent PCB 136 away from the sites of PCB metabolism due to hepatic sequestration. Similarly, we have suggested that the less pronounced atropisomeric enrichment of (+)-PCB 136 in mice exposed to racemic PCB 136 by intraperitoneal injection compared to oral gavage is due to the sequestration of the PCBs in the peritoneal cavity following intraperitoneal administration.[42]

The observation that PCB 136 undergoes species-dependent atropisomeric enrichment has implications for the selection of animal models for toxicity studies with PCB 136. Several reports demonstrate that chiral PCBs have atropselective interaction with hepatic cytochrome P450 enzymes,[61] atropselectively affect the expression of xenobiotic processing genes in the liver,[62,63] and atropselective metabolism of PCBs to OH-PCBs.[13,48] Moreover, pure PCB atropisomers differentially affect endpoints implicated in the neurodevelopmental toxicity of PCBs.[62,64,65] For example, E_1-(−)-PCB 136, but not E_2-(+)-PCB 136 atropselectively alters morphometric and functional parameters of neuronal connectivity in cultured rat hippocampal neurons. These atropselective effects are mediated by the ryanodine receptor,[66,67] an intracellular calcium channel that has been implicated in the mode of action of PCB-induced developmental neurotoxicity.[25] Several other chiral PCB congeners also affect endpoints implicated in PCB-mediated neurotoxicity in an atropselective manner.[64,65]

Atropisomeric enrichment of PCB 136 metabolites in whole blood.

The direction and extent of the atropisomeric enrichment of two metabolites, 4–136 and 5–136, were determined at the 5 h time point only. The atropisomer of 4–136 eluting second on the CB column (E_2-4–136) and the atropisomer of 5–135 eluting first on the CD column (E_1-5–136) were enriched in whole blood from all exposure groups (Figure 4; Table S5). The same direction of atropisomeric enrichment was observed for both PCB 136 metabolites in our earlier study in the same mouse model.[33] E_1-5–136 is also formed preferentially in metabolism studies with racemic PCB 136 in mouse liver microsomes and precision cut liver tissue slices. In contrast, E_1-4–136 was formed preferentially in the *in vitro* model systems, an observation that suggests that the atropisomeric enrichment of chiral OH-PCB metabolites *in vivo* is determined by more complex metabolic processes, including further metabolism to dihydroxylated PCBs, PCB sulfates, PCB glucuronides, PCB glutathione conjugates, and other metabolites.[13]

More pronounced atropisomeric enrichment was observed at 5 h post exposure for 4–136 and 5–135 in WT compared to KO mice; however, this difference reached statistical significance only in female mice (Figure 6B and 6C). Similarly, F-WT displayed a significantly more pronounced atropisomeric enrichment of E_2-4–136 compared to F-KO

mice in our previous study.[33] This observation is consistent with an impaired hepatic metabolism in KO mice; however, atropselective conjugation of the OH-PCBs to sulfate or glucuronide metabolites may also contribute to the EF values observed in KO *vs.* WT mice.[27] In contrast to the 5 h time point investigated in this study, 5–136 appeared to be near racemic in F-WT mice (EF = 0.47) compared to F-KO mice (EF = 0.31) 72 h after PCB 136 exposure.[33] As discussed above, the difference in the enrichment of 5–136 atropisomers between both studies may be due to the different time points or the different PCB 136 doses investigated.

Toxicokinetic parameters of PCB 136 and its metabolites in whole blood.

To gain additional insights into the disposition of PCB 136 atropisomers and its metabolites in KO *vs.* WT mice, several toxicokinetic parameters were determined with Monte Carlo simulations. Several parameters, including C_{max}, AUC24, AUC24ss, and SSa, showed differences depending on genotype and sex (Figure 7). Other parameters, such as T_{max} and, surprisingly, $t_{1/2}$ showed no statistically significant differences (Figure S1). The lack of a significant difference in $t_{1/2}$ for both PCB 136 atropisomers is surprising because of the pronounced atropisomeric enrichment of (+)-PCB 136. However, an earlier toxicokinetics study also observed no significant difference in the terminal half-life of first *vs.* second elution PCB atropisomers in mice exposed to an environmental mixture of eight chiral PCB congeners.[55] These observations indicate that the experimental error of the $t_{1/2}$ determination for both PCB 136 atropisomers is relatively large, most likely because of the destructive sampling approach used in both studies.

The maximum concentration, C_{max}, for both PCB 136 atropisomers and two metabolites, 5–136 and 4,5–136, were higher in M-WT and F-WT mice compared to the respective KO mice. This difference reached statistical significance only for 4,5–136 in M-WT *vs.* M-KO mice (Figure 7A). The higher C_{max} values for PCB 136 atropisomers in WT mice may be due to the higher fat content of the liver of KO compared to WT mice,[31,33] which results in the hepatic sequestration of the PCB 136 and reduces the quantity of PCB 136 that reaches the systemic circulation in KO mice. We also noted small sex differences in C_{max} of 4–136 and 5–136; however, these differences did not reach statistical significance (Table S4). C_{max} was higher for (+)-136 than (−)-PCB 136 in all four exposure groups, which is consistent with the enrichment of (+)-PCB 136 in this and other studies;[68,69] however, this difference was not statistically significant. T_{max}, the time to reach C_{max}, was longer for 4–136 and 4,5–136 compared to the PCB 136 atropisomers and 5–136. The later observation is not surprising because 4,5–136 is likely formed by oxidation of 5–136 and 4–136, as suggested by *in vitro* metabolism studies with other OH-PCBs.[34,61,70]

The AUC24 and AUC24ss for both PCB 136 atropisomers and two of its metabolites, 5–136 and 4,5–136, were higher in M-WT *vs.* M-KO mice (Figure 7C and 7D, respectively; Table S4). This difference reached statistical significance for (+)-PCB 136, 5–136 and 4,5–136 for AUC24 and 5–136 and 4,5–136 for AUC24ss. Similarly, the AUC24 for these three compounds were higher in F-WT *vs.* F-KO mice; however, this difference reached statistical significance only for 4,5–136. In contrast, no significant differences in the AUC24ss were observed when comparing F-KO and F-WT mice. In addition to differences by genotype, we

observed some differences in both toxicokinetic parameters by sex. Briefly, the AUC24ss for PCB 136 and 4,5–136 was significantly higher in M-WT *vs.* F-WT mice. The opposite trend was observed for PCB 136, 5–136 and 4,5–136 in KO, with AUC24ss values being lower in M-KO *vs.* F-KO mice. This difference reached statistical significance for 5–136. The sex and genotype-dependent differences in AUC24 and AUC24ss are consistent with the differences in the molar percentages of ∑OH-PCBs and PCB 136 discussed above (Figure 3).

The steady-state degree of accumulation, SSa, was determined to assess the extent of accumulation of PCB 136 and its hydroxylated metabolites in the blood (Figures 7G and 7H). 4–136 in male and female mice and 4,5–136 in male mice displayed a higher degree of accumulation in blood under steadystate conditions compared to both PCB 136 atropisomers and 5–136. This observation is not entirely surprising because some *para* hydroxylated PCB metabolites are typically more persistent in mammals, including humans,[71] whereas *meta* hydroxylated metabolites, such as 5–136, are more readily excreted in mice.[33] In addition to these metabolite specific differences, the SSa displayed differences depending on the genotype and sex. Briefly, the SSa for PCB 136, 5–136, and 4,5–136 was higher in M-KO and F-KO mice compared to the corresponding WT mice. This difference reached statistical significance for both PCB 136 atropisomers and 5–136 in female mice (Table S4). Moreover, M-KO mice displayed a higher degree of accumulation of PCB 136, 5–136 and 4,5–136 compared to F-KO mice. The SSa values for PCB 136 and its metabolites were lower in F-WT mice compared to M-WT mice.

These findings demonstrate that the liver-specific deletion of the *cpr* gene affects levels and the atropisomeric enrichment of PCB 136 in a sex and genotype-dependent manner and alters the profiles and chiral signatures of OH-PCB 136 metabolites over time, both after a single acute exposure or at steady state. These differences in blood profiles, levels, and chiral signatures are expected to translate into differences in the toxicokinetics and, ultimately, toxicodynamics, in target organs from KO *vs.* WT mice. As discussed above, several changes resulting from the liver-specific deletion of the *cpr* gene likely contribute to the differences in the toxicokinetics of PCB 136 and its metabolites in KO compared to WT mice. These changes include an impaired hepatic oxidation of PCB 136 to OH-PCBs; compensatory changes in the expression of other drug metabolizing enzymes in the liver and other organs; and the increased fat content in the liver. Although multiple factors contribute to the altered disposition of PCB 136 and its metabolites in KO compared WT mice, mice with a liver-specific deletion of the *cpr* gene are one mouse model that could be used to assess how impaired hepatic metabolism affect neurotoxic outcomes in mice exposed throughout development to PCBs. Thus, KO mice with a liver-specific deletion of the *cpr* gene are a relevant model for toxicity studies of PCBs and their metabolites.

Supplementary Material

Refer to Web version on PubMed Central for supplementary material.

ACKNOWackLEDGMENT

The authors would thank Dr. Xinxin Ding of the University of Arizona (Tucson, Arizona) for providing the mouse model. The PCB 136 derivatives were a generous gift from E.A. Mash and S.C. Waller of the Synthetic Chemistry Facility Core of the Southwest Environmental Health Sciences Center.

Funding Sources

The project was supported by grants ES05605, ES013661, and ES027169 from the National Institute of Environmental Health Science/National Institutes of Health. The synthesis of several PCB 136 metabolite standards was funded by NIH grant ES06694. The content is solely the responsibility of the authors and does not necessarily represent the official views of the National Institute of Environmental Health Sciences or the National Institutes of Health.

ABBREVIATIONS

PCB	polychlorinated biphenyls
cpr	cytochrome P450 reductase
CD column	Chiralsil-Dex CB column
CB column	Cylcosil-B column
PCB 136	2,2', 3,3',6,6'-hexachlorobiphenyl
KO	knockout
WT	wild type
EF	enantiomeric fraction
3–150	2,2′,3′,4,6,6′-hexachlorobiphenyl-3-ol
4–136	2,2′,3,3′,6,6′-hexachlorobiphenyl-4-ol
5–136	2,2′,3,3′,6,6′-hexachlorobiphenyl-5-ol
4,5–136	4,5-dihydroxy-2,2′,3,3′,6,6′-hexachlorobiphenyl

REFERENCES

(1). ATSDR. (2017) ATSDR's substance priority list, https://www.atsdr.cdc.gov/spl/.

(2). Xiao P, Zhao YX, Wang T, Zhan YY, Wang HH, Li JL, Thomas A, and Zhu JJ (2014) Polymeric carbon nitride/mesoporous silica composites as catalyst support for Au and Pt nanoparticles. Chem. Eur J 20, 2872–2878. [PubMed: 24497094]

(3). Herkert NJ, Jahnke JC, and Hornbuckle KC (2018) Emissions of tetrachlorobiphenyls (PCBs 47, 51, and 68) from polymer resin on kitchen cabinets as a non-Aroclor source to residential air. Environ. Sci. Technol 52, 5154–5160. [PubMed: 29667399]

(4). Anezaki K, and Nakano T (2014) Concentration levels and congener profiles of polychlorinated biphenyls, pentachlorobenzene, and hexachlorobenzene in commercial pigments. Environ. Sci. Pollut. Res 21, 998–1009.

(5). Hu D, and Hornbuckle KC (2010) Inadvertent polychlorinated biphenyls in commercial paint pigments. Environ. Sci. Technol 44, 2822–2827. [PubMed: 19957996]

(6). ATSDR. Toxicological Profile for Polychlorinated Biphenyls (PCBs) https://www.atsdr.cdc.gov/toxprofiles/tp.asp?id=142&tid=26.

(7). Hansen LG (1999) The ortho side of PCBs: Occurrence and disposition Kluwer Academic Publishers, Boston.

(8). Harrad S, Ren JZ, and Hazrati S (2006) Chiral signatures of PCB#s 95 and 149 in indoor air, grass, duplicate diets and human faeces. Chemosphere 63, 1368–1376. [PubMed: 16289232]

(9). Schecter A, Colacino J, Haffner D, Patel K, Opel M, Papke O, and Birnbaum L (2010) Perfluorinated compounds, polychlorinated biphenyls, and organochlorine pesticide contamination in composite food samples from Dallas, Texas, USA. Environ. Health. Persp 118, 796–802.

(10). Shin ES, Nguyen KH, Kim J, Kim CI, and Chang YS (2015) Progressive risk assessment of polychlorinated biphenyls through a total diet study in the Korean population. Environ. Pollut 207, 403–412. [PubMed: 26470055]

(11). Marek RF, Thome PS, Herkert NJ, Awad AM, and Hornbuckle KC (2017) Airborne PCBs and OH-PCBs Inside and Outside Urban and Rural US Schools. Environ. Sci. Technol 51, 7853–7860. [PubMed: 28656752]

(12). Herrick RF, Stewart JH, and Allen JG (2016) Review of PCBs in US schools: a brief history, an estimate of the number of impacted schools, and an approach for evaluating indoor air samples. Environ. Sci. Pollut. Res 23, 1975–1985.

(13). Grimm FA, Hu D, Kania-Korwel I, Lehmler HJ, Ludewig G, Hornbuckle KC, Duffel MW, Bergman A, and Robertson LW (2015) Metabolism and metabolites of polychlorinated biphenyls. Crit. Rev. Toxicol 45, 245–272. [PubMed: 25629923]

(14). Herrick RF, Meeker JD, and Altshul L (2011) Serum PCB levels and congener profiles among teachers in PCB-containing schools: a pilot study. Environ. Health 10.

(15). Jamshidi A, Hunter S, Hazrati S, and Harrad S (2007) Concentrations and chiral signatures of polychlorinated biphenyls in outdoor and indoor air and soil in a major UK conurbation. Environ. Sci. Technol 41, 2153–2158. [PubMed: 17438756]

(16). Currado GM, and Harrad S (1998) Comparison of polychlorinated biphenyl concentrations in indoor and outdoor air and the potential significance of inhalation as a human exposure pathway. Environ. Sci. Technol 32, 3043–3047.

(17). Fromme H, Baldauf AM, Klautke O, Piloty M, and Bohrer L (1996) Polychlorinated biphenyls (PCB) in caulking compounds of buildings-assessment of current status in berlin and new indoor air sources. Gesundheitswesen 58, 666–672. [PubMed: 9081511]

(18). Thomas K, Xue J, Williams R, Jones P, and Whitaker D (2012) Polychlorinated biphenyls (PCBs) in school buildings: sources, environmental levels, and exposures, United States Environmental Protection Agency, Office of Research and Development, National Exposure Research Laboratory, https://www.epa.gov/sites/production/files/2015-08/documents/pcb_epa600r12051_final.pdf.

(19). Winneke G (2011) Developmental aspects of environmental neurotoxicology: Lessons from lead and polychlorinated biphenyls. J. Neurol. Sci 308, 9–15. [PubMed: 21679971]

(20). Korrick SA, and Sagiv SK (2008) Polychlorinated biphenyls, organochlorine pesticides and neurodevelopment. Curr. Opin. Pediatr 20, 198–204. [PubMed: 18332718]

(21). Schantz SL, Widholm JJ, and Rice DC (2003) Effects of PCB exposure on neuropsychological function in children. Environ. Health. Persp 111, 357–376.

(22). Wayman GA, Yang DR, Bose DD, Lesiak A, Ledoux V, Bruun D, Pessah IN, and Lein PJ (2012) PCB 95 promotes dendritic growth via ryanodine receptor-dependent mechanisms. Environ. Health. Persp 120, 997–1002.

(23). Yang D, Kim KH, Phimister A, Bachstetter AD, Ward TR, Stackman RW, Mervis RF, Wisniewski AB, Klein SL, Kodavanti PRS, Anderson KA, Wayman G, Pessah IN, and Lein PJ (2009) Developmental exposure to polychlorinated biphenyls interferes with experience-dependent dendritic plasticity and ryanodine receptor expression in weanling rats. Environ. Health. Persp 117, 426–435.

(24). Schantz SL, Seo BW, Wong PW, and Pessah IN (1997) Long-term effects of developmental exposure to 2,2',3,5',6-pentachlorobiphenyl (PCB 95) on locomotor activity, spatial learning and memory and brain ryanodine binding. Neurotoxicology 18, 457–467. [PubMed: 9291494]

(25). Pessah IN, Cherednichenko G, and Lein PJ (2010) Minding the calcium store: Ryanodine receptor activation as a convergent mechanism of PCB toxicity. Pharmacol. Ther 125, 260–285. [PubMed: 19931307]

(26). Lesiak A, Zhu M, Chen H, Appleyard SM, Impey S, Lein PJ, and Wayman GA (2014) The environmental neurotoxicant PCB 95 promotes synaptogenesis via ryanodine receptor-dependent miR132 upregulation. J. Neurosci 34, 717–725. [PubMed: 24431430]

(27). Kania-Korwel I, and Lehmler HJ (2016) Chiral polychlorinated biphenyls: absorption, metabolism and excretion-a review. Environ. Sci. Pollut. Res. Int 23, 2042–2057. [PubMed: 25651810]

(28). Kania-Korwel I, Lukasiewicz T, Barnhart CD, Stamou M, Chung H, Kelly KM, Bandiera S, Lein PJ, and Lehmler HJ (2017) Editor's highlight: Congener-specific disposition of chiral polychlorinated biphenyls in lactating mice and their offspring: Implications for PCB developmental neurotoxicity. Toxicol. Sci 158, 101–115. [PubMed: 28431184]

(29). Niknam Y, Feng W, Cherednichenko G, Dong Y, Joshi SN, Vyas SM, Lehmler H-J, and Pessah IN (2013) Structure-activity relationship of select meta- and para-hydroxylated non-dioxin-like polychlorinated biphenyls: from single RyR1 channels to muscle dysfunction. Toxicol. Sci 136, 500–513. [PubMed: 24014653]

(30). Pessah IN, Hansen LG, Albertson TE, Garner CE, Ta TA, Do Z, Kim KH, and Wong PW (2006) Structure-activity relationship for noncoplanar polychlorinated biphenyl congeners toward the ryanodine receptor-Ca^{2+} channel complex type 1 (RyR1). Chem. Res. Toxicol 19, 92–101. [PubMed: 16411661]

(31). Wu L, Gu J, Weng Y, Kluetzman K, Swiatek P, Behr M, Zhang QY, Zhuo XL, Xie Q, and Ding XX (2003) Conditional knockout of the mouse NADPH-cytochrome p450 reductase gene. Genesis 36, 177–181. [PubMed: 12929087]

(32). Gu J, Weng Y, Zhang Q, Cui H, Behr M, Wu L, Yang W, Zhang L, and Ding X (2003) Liver-specific deletion of the NADPH-cytochrome P450 reductase gene - Impact on plasma cholesterol homeostasis and the function and regulation of microsomal cytochrome P450 and heme oxygenase. J. Biol. Chem 278, 25895–25901. [PubMed: 12697746]

(33). Wu X, Barnhart C, Lein PJ, and Lehmler HJ (2015) Hepatic metabolism affects the atropselective disposition of 2,2',3,3',6,6'-hexachlorobiphenyl (PCB 136) in mice. Environ. Sci. Technol 49, 616–625. [PubMed: 25420130]

(34). Waller SC, He YA, Harlow GR, He YQ, Mash EA, and Halpert JR (1999) 2,2',3,3',6,6'-hexachlorobiphenyl hydroxylation by active site mutants of cytochrome P4502B1 and 2B11. Chem. Res. Toxicol 12, 690–699. [PubMed: 10458702]

(35). Kania-Korwel I, Vyas SM, Song Y, and Lehmler HJ (2008) Gas chromatographic separation of methoxylated polychlorinated biphenyl atropisomers. J. Chromatogr. A 1207, 146–154. [PubMed: 18760792]

(36). Black TH (1982) The preparation and reactions of diazomethane. Aldrichimica Acta 15, 3–10.

(37). Wong PW, Joy RM, Albertson TE, Schantz SL, and Pessah IN (1997) Ortho-substituted 2,2',3,5', 6-pentachlorobiphenyl (PCB 95) alters rat hippocampal ryanodine receptors and neuroplasticity in vitro: Evidence for altered hippocampal function. Neurotoxicology 18, 443–456. [PubMed: 9291493]

(38). Pessah IN, Hansen LG, Albertson TE, Garner CE, Ta TA, Do Z, Kim KH, and Wong PW (2006) Structure-activity relationship for noncoplanar polychlorinated biphenyl congeners toward the ryanodine receptor-Ca2+ channel complex type 1 (RyR1). Chem. Res. Toxicol 19, 92–101. [PubMed: 16411661]

(39). Simon T, Britt JK, and James RC (2007) Development of a neurotoxic equivalence scheme of relative potency for assessing the risk of PCB mixtures. Regul. Toxico.l Pharm 48, 148–170.

(40). Wu X, Kammerer A, and Lehmler HJ (2014) Microsomal oxidation of 2,2',3,3',6,6'-hexachlorobiphenyl (PCB 136) results in species-dependent chiral signatures of the hydroxylated metabolites. Environ. Sci. Technol 48, 2436–2444. [PubMed: 24467194]

(41). Wu X, Pramanik A, Duffel MW, Hrycay EG, Bandiera SM, Lehmler HJ, and Kania-Korwel I (2011) 2,2',3,3',6,6'-Hexachlorobiphenyl (PCB 136) is enantioselectively oxidized to

hydroxylated metabolites by rat liver microsomes. Chem. Res. Toxicol 24, 2249–2257. [PubMed: 22026639]

(42). Kania-Korwel I, Shaikh NS, Hornbuckle KC, Robertson LW, and Lehmler HJ (2007) Enantioselective disposition of PCB 136 (2,2',3,3',6,6'-hexachlorobiphenyl) in C57BL/6 mice after oral and intraperitoneal administration. Chirality 19, 56–66. [PubMed: 17089340]

(43). Kania-Korwel I, Duffel MW, and Lehmler HJ (2011) Gas chromatographic analysis with chiral cyclodextrin phases reveals the enantioselective formation of hydroxylated polychlorinated biphenyls by rat liver microsomes. Environ. Sci. Technol 45, 9590–9596. [PubMed: 21966948]

(44). Kania-Korwel I, Barnhart CD, Lein PJ, and Lehmler HJ (2015) Effect of pregnancy on the disposition of 2,2',3,5',6-pentachlorobiphenyl (PCB 95) atropisomers and their hydroxylated metabolites in female mice. Chem. Res. Toxicol 28, 1774–1783. [PubMed: 26271003]

(45). Kania-Korwel I, and Lehmler HJ (2013) Assigning atropisomer elution orders using atropisomerically enriched polychlorinated biphenyl fractions generated by microsomal metabolism. J. Chromatogr. A 1278, 133–144. [PubMed: 23347976]

(46). Haglund P, and Wiberg K (1996) Determination of the gas chromatographic elution sequences of the (+)- and (−)-enantiomers of stable atropisomeric PCBs on chirasil-dex. J. High Resol. Chromatogr 19, 373–376.

(47). (2013) Base SAS® 9.4 procedures guide: statistical procedures Second Edition ed., SAS Institute Inc., Cary, NC, USA.

(48). Kania-Korwel I, and Lehmler HJ (2016) Toxicokinetics of chiral polychlorinated biphenyls across different species-a review. Environ. Sci. Pollut. Res. Int 23, 2058–2080. [PubMed: 25824003]

(49). Lehmler HJ, Harrad SJ, Huhnerfuss H, Kania-Korwel I, Lee CM, Lu Z, and Wong CS (2010) Chiral polychlorinated biphenyl transport, metabolism, and distribution: a review. Environ. Sci. Technol 44, 2757–2766. [PubMed: 20384371]

(50). Cheng XG, Gu J, and Klaassen CD (2014) Adaptive hepatic and intestinal alterations in mice after deletion of NADPH-cytochrome P450 oxidoreductase (cpr) in hepatocytes. Drug. Metab. Dispos 42, 1826–1833. [PubMed: 25147274]

(51). Ptak A, Ludewig G, Kapiszewska M, Magnowska Z, Lehmer HJ, Robertson LW, and Gregoraszczuk EL (2006) Induction of cytochromes P450, caspase-3 and DNA damage by PCB3 and its hydroxylated metabolites in porcine ovary. Toxicol. Lett 166, 200–211. [PubMed: 16949219]

(52). Xie W, Wang K, Robertson LW, and Ludewig G (2010) Investigation of mechanism(s) of DNA damage induced by 4-monochlorobiphenyl (PCB 3) metabolites. Environ. Int 36, 950–961. [PubMed: 20129669]

(53). Kania-Korwel I, Xie W, Hornbuckle KC, Robertson LW, and Lehmler HJ (2008) Enantiomeric enrichment of 2,2 ‘,3,3 ‘,6,6 ‘-hexachlorobiphenyl (PCB 136) in mice after induction of CYP enzymes. Arch Environ. Contam. Toxicol 55, 510–517. [PubMed: 18437444]

(54). Kania-Korwel I, Hornbuckle KC, Robertson LW, and Lehmler HJ (2008) Dose-dependent enantiomeric enrichment of 2,2',3,3',6,6'-hexachlorobiphenyl in female mice. Environ. Toxicol. Chem 27, 299–305. [PubMed: 18348647]

(55). Kania-Korwel I, El-Komy MH, Veng-Pedersen P, and Lehmler HJ (2010) Clearance of polychlorinated biphenyl atropisomers is enantioselective in female C57BL/6 mice. Environ. Sci. Technol 44, 2828–2835. [PubMed: 20384376]

(56). Milanowski B, Lulek J, Lehmler HJ, and Kania-Korwel I (2010) Assessment of the disposition of chiral polychlorinated biphenyls in female mdr 1a/b knockout versus wild-type mice using multivariate analyses. Environ. Int 36, 884–892. [PubMed: 19923000]

(57). Wu X, Kania-Korwel I, Chen H, Stamou M, Dammanahalli KJ, Duffel M, Lein PJ, and Lehmler HJ (2013) Metabolism of 2,2',3,3',6,6'-hexachlorobiphenyl (PCB 136) atropisomers in tissue slices from phenobarbital or dexamethasone-induced rats is sex-dependent. Xenobiotica 43, 933–947. [PubMed: 23581876]

(58). Wu X, Yang J, Morisseau C, Robertson LW, Hammock B, and Lehmler HJ (2016) 3,3',4,4',5-Pentachlorobiphenyl (PCB 126) decreases hepatic and systemic ratios of epoxide to diol

metabolites of unsaturated fatty acids in male rats. Toxicol. Sci 152, 309–322. [PubMed: 27208083]

(59). Van Birgelen APJM, Vanderkolk J, Fase KM, Bol I, Poiger H, Brouwer A, and Vandenberg M (1994) Toxic potency of 3,3',4,4',5-pentachlorobiphenyl relative to and in combination with 2,3,7,8-tetrachlorodibenzo-p-dioxin in a subchronic feeding study in the rat. Toxicol. Appl. Pharm 127, 209–221.

(60). Chu I, Villeneuve DC, Yagminas A, Lecavalier P, Poon R, Feeley M, Kennedy SW, Seegal RF, Hakansson H, Ahlborg UG, and Valli VE (1994) Subchronic toxicity of 3,3',4,4',5-pentachlorobiphenyl in the rat .1. clinical, biochemical, hematological, and histopathological changes. Fund. Appl. Toxicol 22, 457–468.

(61). Lu Z, Kania-Korwel I, Lehmler HJ, and Wong CS (2013) Stereoselective Formation of Mono- and Dihydroxylated Polychlorinated Biphenyls by Rat Cytochrome P450 2B1. Environ. Sci. Technol 47, 12184–12192. [PubMed: 24060104]

(62). Pencikova K, Brenerova P, Svrzkova L, Hruba E, Palkova L, Vondracek J, Lehmler HJ, and Machala M (2018) Atropisomers of 2,2',3,3 ,6,6'-hexachlorobiphenyl (PCB 136) exhibit stereoselective effects on activation of nuclear receptors in vitro. Environ. Sci. Pollut. Res 25, 16411–16419.

(63). Puttmann M, Mannschreck A, Oesch F, and Robertson L (1989) Chiral effects in the induction of drug-metabolizing-enzymes using synthetic atropisomers of polychlorinated-biphenyls (PCBs). Biochem. Pharmacol 38, 1345–1352. [PubMed: 2495802]

(64). Feng W, Zheng J, Robin G, Dong Y, Ichikawa M, Inoue Y, Mori T, Nakano T, and Pessah IN (2017) Enantioselectivity of 2,2',3,5',6-pentachlorobiphenyl (PCB 95) atropisomers toward ryanodine receptors (RyRs) and their influences on hippocampal neuronal networks. Environ. Sci. Technol 51, 14406–14416. [PubMed: 29131945]

(65). Lehmler HJ, Robertson LW, Garrison AW, and Kodavanti PR (2005) Effects of PCB 84 enantiomers on [^{3}H] phorbol ester binding in rat cerebellar granule cells and $^{45}Ca^{2+}$-uptake in rat cerebellum. Toxicol. Lett 156, 391–400. [PubMed: 15763638]

(66). Pessah IN, Lehmler HJ, Robertson LW, Perez CF, Cabrales E, Bose DD, and Feng W (2009) Enantiomeric specificity of (−)-2,2',3,3',6,6'-hexachlorobiphenyl toward ryanodine receptor types 1 and 2. Chem. Res. Toxicol 22, 201–207. [PubMed: 18954145]

(67). Yang D, Kania-Korwel I, Ghogha A, Chen H, Stamou M, Bose DD, Pessah IN, Lehmler HJ, and Lein PJ (2014) PCB 136 atropselectively alters morphometric and functional parameters of neuronal connectivity in cultured rat hippocampal neurons via ryanodine receptor-dependent mechanisms. Toxicol. Sci 138, 379–392. [PubMed: 24385416]

(68). Lehmler H-J, Harrad SJ, Huhnerfuss H, Kania-Korwel I, Lee CM, Lu Z, and Wong CS (2010) Chiral polychlorinated biphenyl transport, metabolism, and distribution: A review. Environ. Sci. Technol 44, 2757–2766. [PubMed: 20384371]

(69). Kania-Korwel I, and Lehmler HJ (2016) Chiral polychlorinated biphenyls: absorption, metabolism and excretion-a review. Environ. Sci. Pollut. Res. Int 23, 2042–2057. [PubMed: 25651810]

(70). McLean MR, Bauer U, Amaro AR, and Robertson LW (1996) Identification of catechol and hydroquinone metabolites of 4-monochlorobiphenyl. Chem. Res. Toxicol 9, 158–164. [PubMed: 8924585]

(71). Bergman A, Klassonwehler E, and Kuroki H (1994) Selective retention of hydroxylated PCB metabolites in blood. Environ. Health. Persp 102, 464–469.

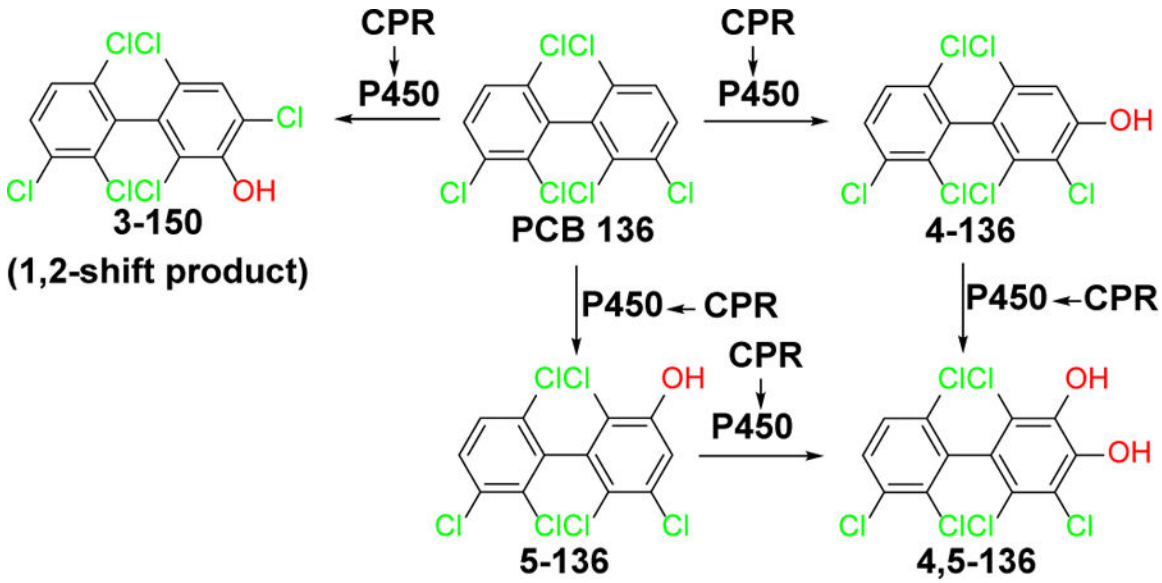

Figure 1.

PCB 136 is metabolized to mono- and dihydroxylated metabolites by cytochrome P450 (P450) enzymes. Microsomal P450 enzymes require CPR as the electron donor for oxidation reactions. CPR is not expressed in the liver of KO mice.

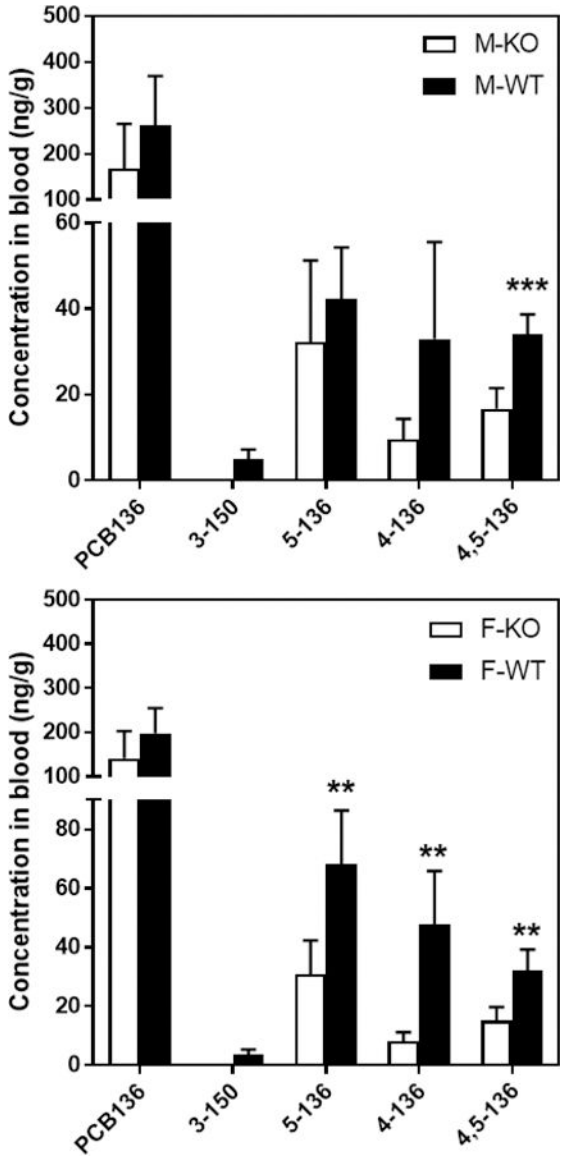

Figure 2.

Comparison of levels of PCB 136 and its hydroxylated metabolites between KO and WT mice in whole blood from (a) male and (b) female mice collected 5 h after oral exposure to racemic PCB 136 (M-KO, n = 6; M-WT, n = 6; F-KO, n = 5, F-WT, n = 5). Significant difference from KO; *** $p < 0.001$; ** $p < 0.01$. Values are presented as mean ± standard deviation.

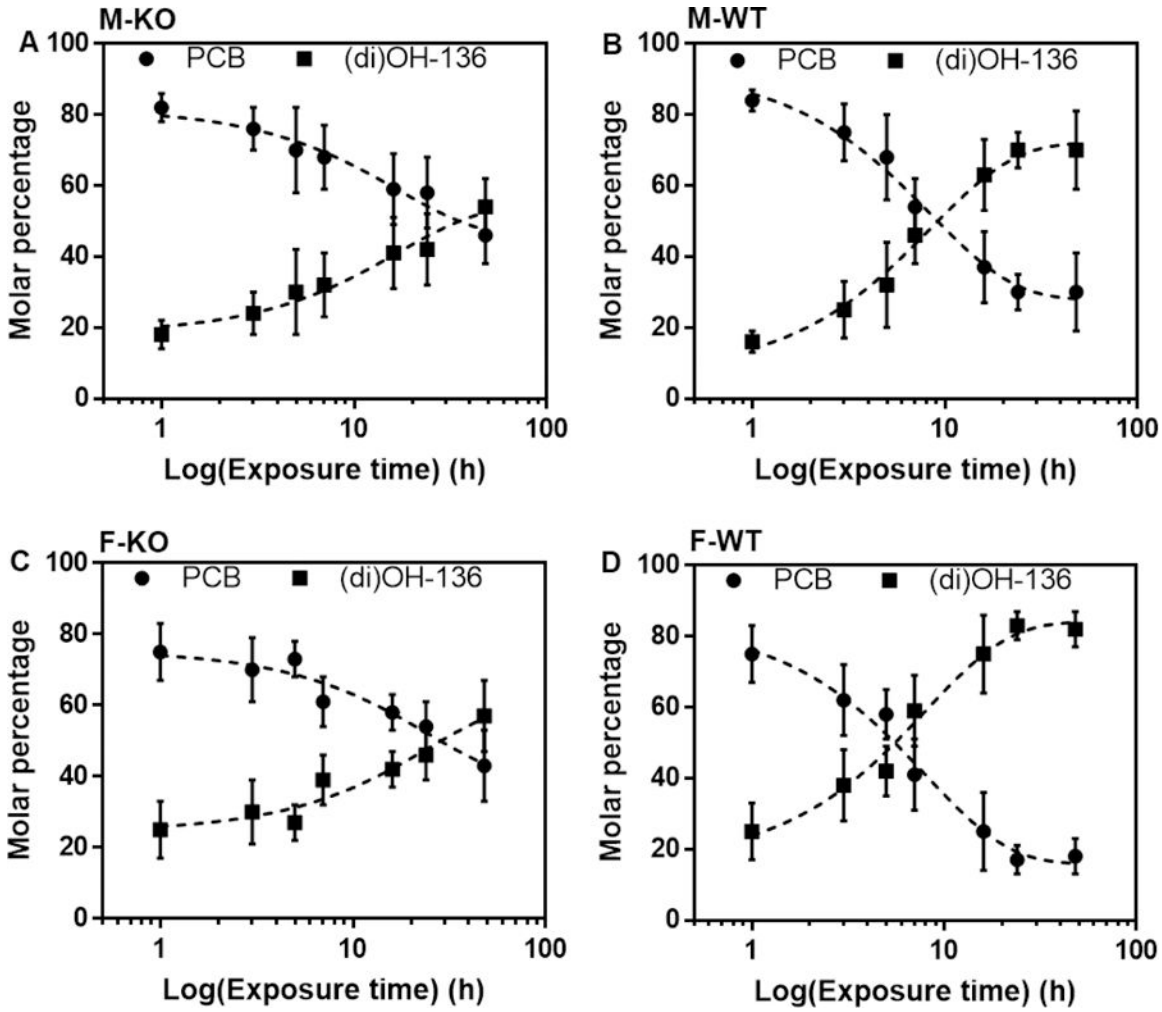

Figure 3.

The molar percentage of PCB 136 and the sum of hydroxylated metabolites, ΣHO-PCBs, changed over exposure time in whole blood from (A) male KO (M-KO), (B) male wildtype (M-WT), (C) female KO (F-KO), (D) female wildtype (F-WT) mice. The dotted lines are trendlines added to visualize the change of the molar percentage of PCB 136 vs. ΣHO-PCBs in mouse blood over time. The molar percentages of PCBs and OH-PCBs were calculated from the sum of the PCB and OH-PCB levels in the whole blood from each animal and subsequently averaged for all animals within the exposure group.

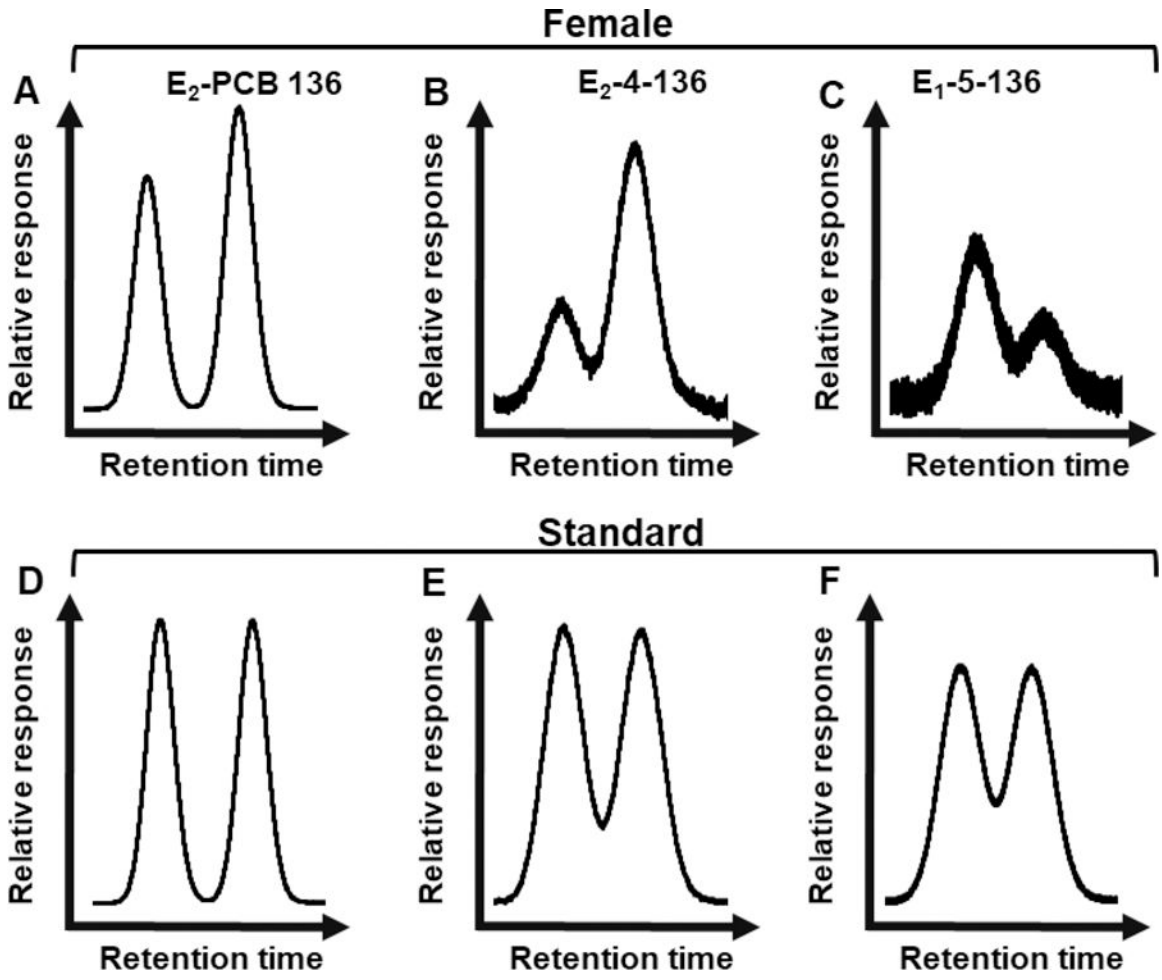

Figure 4.

Representative gas chromatograms showing the atropisomeric enrichment of (A) E_2-PCB 136, (B) E_2-4–136 and (C) E_1-5–136 in whole blood from a female wild-type (F-WT) mice. Gas chromatograms of racemic standards of (D) PCB 136, (E) 4–136 and (F) 5–136 are shown for comparison. Whole blood was collected from mice 5 h after oral exposure racemic PCB 136. Extracts were analyzed on CD (PCB 136 and 5–136) and CB (4–136) capillary columns as described under Experimental Procedures. The x- and y-axis show the relative retention times of the atropisomers on the respective chiral column and the relative response of the ^{63}Ni-μECD detector used for the atropselective analyses, respectively.

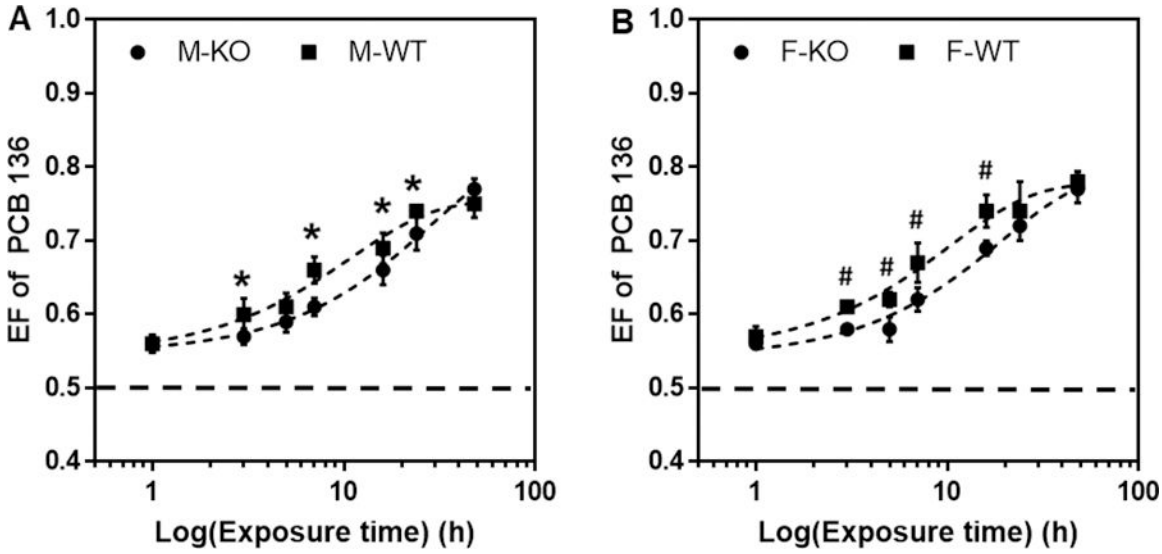

Figure 5.

The enantiomeric fraction (EF) of PCB 136 in whole blood from (A) male KO (M-KO) and male WT (M-WT), and (B) female KO (F-KO), and female WT (F-WT) mice increased over time, with (+)-PCB 136 being enriched in all exposure groups at all time points. Animals were euthanized 1 to 48 h following oral exposure to racemic PCB 136 (n = 3 to 6), PCB 136 was extracted from whole blood, and enantiomeric fractions were determined using a CD column (see Experimental Procedures). EF values were calculated based on the equation EF = Area E_2/(Area E_1+Area E_2) and are presented as the mean ± standard deviation. For a summary of the EF values, see Table S6. *: Significant difference from M-WT ($p < 0.05$), #: Significant difference from F-WT ($p < 0.05$). All EF values were significantly different from the EF values of the racemic PCB 136 standard (EF = 0.501 ± 0.003, n = 11).

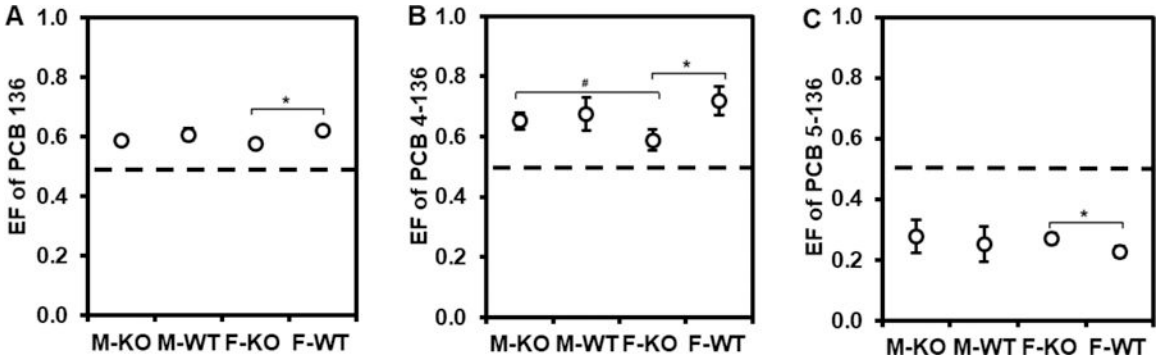

Figure 6.

Comparison of enantiomeric fractions (EFs) of (a) PCB 136, (b) 4–136 and (c) 5–136 in whole blood from male and female KO and WT mice exposed to racemic PCB 136. Whole blood was collected 5 h after oral exposure to racemic PCB 136 (n = 3–6). Extracts were analyzed on CD (PCB 136 and 5–136) and CB (4–136) capillary columns as described under Experimental Procedures. EF values were calculated based on the equation EF = Area E_2/(Area E_1+Area E_2) and are presented as the mean ± standard deviation. For a summary of the EF values, see Table S5. *: F-KO is significantly different from F-WT ($p < 0.05$), $^{\#}$: M-KO is significantly different from F-KO ($p < 0.05$). All EF values were significantly different from the EF values of the racemic PCB 136 (EF = 0.501 ± 0.003, n = 11), 4–136 (EF = 0.500 ± 0.003, n = 3) and 5–136 (EF = 0.500 ± 0.003, n = 3) standards.

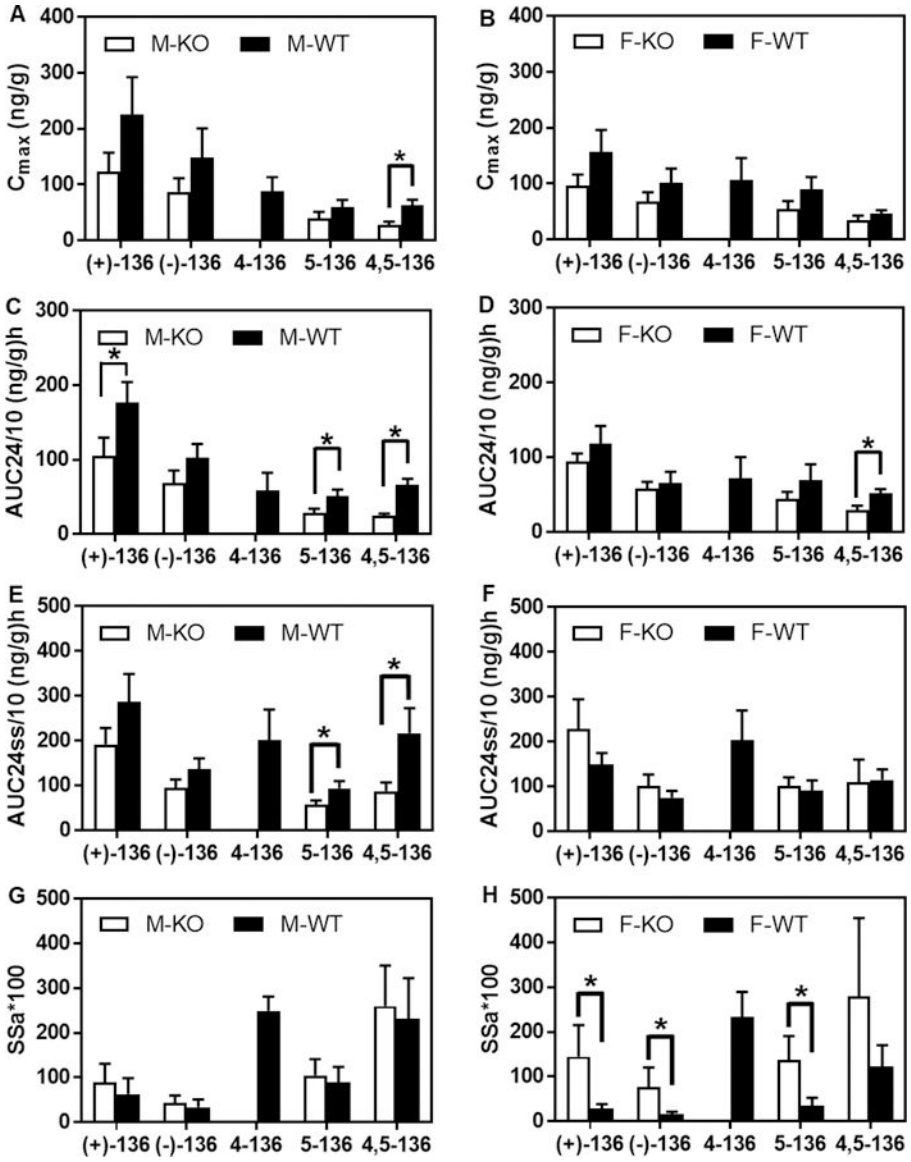

Figure 7.

Comparison of toxicokinetic parameters of PCB 136 and its metabolites in whole blood from KO *vs.* WT mice orally exposed to racemic PCB 136, including the maximum concentration determined from a single administration, C_{max}, of (A) male and (B) female mice; the area under the concentration *vs.* time curve in the interval from zero to 24 hours resulting from a single dose given at time zero, AUC24, of (C) male and (D) female mice; the area under the concentration *vs.* time curve at steady state (SS) in the interval from zero to 24 hours resulting from a single dose given repeatedly every 24 hours, AUC24ss, of (E) male and (F) female mice; the steady state degree of accumulation, SSa, of (G) male and (H) female mice; *Significant difference between the compared pairs ($p < 0.05$). For a detailed summary of the toxicokinetic parameters, see Table S4.